

RESEARCH ARTICLE

WILEY

Influence of sediments burying the discharge area of a karst aquifer on the groundwater flow field—Numerical testing of conceptual models

Marc Ohmer  | Tanja Liesch | Nico Goldscheider

Division of Hydrogeology, Institute of Applied Geosciences, Karlsruhe Institute of Technology, Karlsruhe, Germany

Correspondence

Marc Ohmer, Division of Hydrogeology, Karlsruhe Institute of Technology, Institute of Applied Geosciences, Karlsruhe, Germany.
Email: marc.ohmer@kit.edu

Funding information

Partnership for Research and Innovation in the Mediterranean Area, Grant/Award Number: 01DH19022A

Abstract

Karst springs are a natural result of karst water discharging to the surface through unimpeded pathways where the water table meets the surface. This study investigates the impact of alluvial deposits of varying thicknesses and permeabilities burying the main outlet (karst spring) of a well-developed conduit network on karst drainage, including the development of hydraulic heads, drainage patterns and conduit-matrix interactions in response to a positive base-level shift. Numerical testing using FEFLOW on a simplified conceptual model of a hypothetical karst aquifer with six different model configurations was used to examine various drainage structures (with and without flow through a conduit), spring conditions (free vs. partially/fully clogged), sediment cover thickness (20 and 50 m), and hydraulic conductivity of the sediments (low and high). The numerical testing model incorporated one-dimensional discrete feature elements to simulate conduit flow and coupled conduit-matrix interactions. Results indicate that even with a fully plugged outlet, the conduit network remains a significant contributor to the drainage system, collecting water from the matrix in the recharge zone. As the outlet becomes buried, the hydraulic head increases along the conduit, forcing water back up into the matrix. The elevated hydraulic head in the karst system will cause new conduits to form at the contact between limestone and sediments, creating new potential spring sites (or reactivating existing paleo-phreatic levels). Artesian conditions will occur below the low permeability sediments. These findings provide valuable insights into the responses of natural karst systems.

KEYWORDS

base-level rise, buried karst spring, discrete feature element approach, karst modelling

1 | INTRODUCTION

Karst areas play a vital role as a global water resource while providing valuable ecosystem functions and natural resources (Goldscheider, 2019). The evolution of a karst system is closely linked to the temporal development of the regional base level that guides the regional

orientation of the runoff pattern and controls the main flow gradient. For a mature karst system to develop fast-flowing conduits and caves towards major karst springs, a stable base level for an extended period is necessary. Typically, a base level stability of a few thousand to 100 000 years is needed for karst conduit networks to reach equilibrium (e.g., Bednar, 2000; Dreybrodt, 1990). During this period,

This is an open access article under the terms of the [Creative Commons Attribution](https://creativecommons.org/licenses/by/4.0/) License, which permits use, distribution and reproduction in any medium, provided the original work is properly cited.

© 2023 The Authors. *Hydrological Processes* published by John Wiley & Sons Ltd.

groundwater gradually dissolves soluble rock, creating conduits and caves that facilitate rapid water flow towards spring outlets.

Geomorphological events, often coupled with climatic changes, can swiftly modify boundary conditions at a pace that outstrips speleogenetic processes. For example, a sudden earthquake can rapidly shift the base level of a river, resulting in significant landscape changes within days. Similarly, volcanic eruptions or major landslides can cause abrupt changes to topography and denudation rates (Ford & Williams, 2007). Negative base level shifts caused by tectonic uplift, sea-level fall, or valley deepening by glacial or fluvial erosion can lead to the downward development and rejuvenation of karst networks, while positive shifts caused by filling basins with alluvial, fluvial, lacustrine, glacial or volcanic deposits can cover karst outlets with varying thicknesses of sediment. Additionally, sea-level rise can affect coastal springs due to the resulting increase in water pressure, as denser saltwater can form a barrier to freshwater outflow. Coastal karst systems are particularly vulnerable to these changes, as they are situated at the interface of land and sea (Bakalowicz, 2005; Ford & Williams, 2007).

The following sections will provide a brief overview of three mature karst systems that have undergone a rapid water base-level shift and main outlet plugging with sediments resulting in a notable impact on their present state.

The Messinian salinity crisis, which lasted for approximately 630 000 years during the Late Miocene, is a prominent example of the hydrogeological consequences of a rapid change in groundwater level (Audra et al., 2004; Bakalowicz, 2005). Closure of the Strait of Gibraltar caused the Mediterranean Sea level to drop by up to 1500 m due to evaporation, leading to a significant increase in karstification in the depths of the Mediterranean karst aquifers, with rivers such as the Rhône forming deep valleys. The crisis ended during the Pliocene with the Zanclean flood event, caused by the erosion of the Strait of Gibraltar barrier, which most estimates suggest occurred over a period of several months to several years (García-Castellanos et al., 2009, 2020). The resulting rapid rise in sea level led to the deposition of thick, low-permeability marine and continental sediments in the paleo-valleys, clogging the outlets of Messinian karst systems and leading to an upward migration of springs to reactivated or new discharge points, like the Fontaine de Vaucluse, the prime example and namesake for this spring type. Here, the Messinian Valley of the Rhône, filled with Pliocene deposits, lies up to 900 m below the present sea level (Mocochain et al., 2011). The Messinian conduit system, likely connected to the valley, was buried under impermeable marine sediments. The resulting impounded water and dissolution processes created a 308 m deep vertical chimney in the Fontaine de Vaucluse (Audra et al., 2004).

The Presciano Spring system (PSS) provides another example of the effects of a positive base level shift with subsequent valley aggregation. PSS is a major outlet of the Meso-Cenozoic Gran Sasso fractured karst aquifer, located in the Tirino River Valley (Central Italy). In addition to the impact of the Messinian Crisis, rapid tectonic uplift of the Apennines caused the base flow to move downwards, filling the valleys with recent clastic sediments. Consequently, a dual flow system has evolved, comprising of a fast conduit flow component through buried fractures and conduits originating from the aquifer's core and emerging into the

valley sediments, along with a slow diffusive flow component through the rock matrix (Peleg & Gvirtzman, 2010; Petitta et al., 2015). Groundwater reaches the surface through vertical upwelling in the sediment matrix, forming a 2000 m² seepage area with several large limnogenic springs at the contact zone of the Meso-Cenozoic karst and Quaternary lacustrine deposits (Fiasca et al., 2014). These springs exhibit a relatively constant discharge, which is atypical for karst springs, and possess unique hydrogeological, physicochemical, hydrogeochemical and biological characteristics that suggest the superimposition of a dual groundwater flow system in the local area.

The Donaured gravel aquifer is situated at the geological junction of Germany's most extensive karst aquifer system, the Swabian-Franconian Alb, and the Molasse foreland basin of the Alps. The Swabian Alb underwent significant uplift and deformation during the Cenozoic Era, caused by the Alpine orogeny. In the Tertiary period, the northward-expanding Molasse Sea flooded large parts of the paleokarst landscape and buried them under heterogeneous layers of mostly impermeable molasse sediments. The thickness of these sediments increases rapidly towards the south, reaching several hundred meters in thickness. As a result, the Donaured gravel aquifer, the karst aquifer and the Molasse interact in complex ways, creating various flow paths and mixing multiple water components of different ages from the karst into the gravel-aquifer reservoir (Schloz et al., 2007). Karst groundwater infiltrates the alluvial aquifers in the Danube Valley when: (a) the gravels directly overlay the Jurassic limestones, (b) the low-permeability Molasse sediments have eroded or are thin and (c) vertical upwelling of karst water through Molasse fractures into the alluvial aquifer is possible (Kolokotronis et al., 2002). To identify areas of upwelling karst groundwater, various techniques such as temperature anomalies, chemical analyses and salt dilution tests are employed (Fahrmeier et al., 2021, 2022; Udluft, 2000).

In addition, rapid alterations in karst spring systems may arise from glacial activities, wherein the accumulation of glacier deposits obstructs potential karst springs situated in the low-lying areas of valley flanks. Changes in karst spring systems can occur quickly due to glacial activities that block potential karst springs in low areas of valley flanks with glacier deposits. However, there has been little research on identifying buried springs resulting from this process, likely because it is challenging to identify and study concealed features.

Karst systems are typically studied with a focus on their main drainage through free-draining springs, as evidenced in numerous studies (Bonacci, 2001; Chen & Goldscheider, 2014; Frank et al., 2019; Glennon & Groves, 2002; Jeannin, 2001). However, little is known about karst systems with a sediment-covered discharge zone.

Modelling groundwater flow in karst aquifers is challenging, facing many limitations due to the extreme heterogeneity of hydraulic parameters and the dual flow path regime (Kovács & Sauter, 2007; Scanlon et al., 2003). Therefore, the modelling approach, including the model complexity, varies widely as a function of the research question, depth of process representation and most importantly, the data availability. Lumped parameter models (or reservoir models) are commonly used in studies that aim to understand the dynamic response of karst discharge without considering spatial variability. These models

conceptualize physical processes as a function of linear or nonlinear relationships between storage and discharge at the resolution of the entire aquifer system (Hartmann et al., 2014). However, in recent years, there has been a growing trend towards using data-driven models to simulate karst systems (Lakušić, 2018; Liesch et al., 2021; Paleologos et al., 2013).

Distributed karst models enable the simulation of spatial variability and are classified into three categories: Equivalent Porous Medium Approaches (EPM) (Abusaada & Sauter, 2013; Ghasemizadeh et al., 2015), Double Continuum Approaches (DC) (Bresinsky et al., 2020; Kordilla et al., 2012) and (3) Combined Discrete-Continuum approaches (CDC), which are used in this study. This approach was first applied by Kiraly (1998). The matrix is represented by a continuum formulation, while the conduits are embedded as one-dimensional discrete elements. The best-known codes that implement this approach are MODFLOW with the CFP package (Shoemaker et al., 2008), MODFLOW-USG with the CLN package (Panday et al., 2013) and FEFLOW Discrete Feature Elements (DFN) (Diersch, 2014). This study uses FEFLOW DFN, which has also been utilized in previous studies (e.g., Berglund et al., 2020; Green et al., 2006; Kavouri & Karatzas, 2016; Ninanya et al., 2018).

The primary goal of this study is to explore the hydraulic conditions that emerge in a mature karst system when the base level rises and the main spring outlets become plugged with sediments with varying hydraulic conductivity and thickness. Two specific objectives guide the study:

- To assess the impact of sediment deposition on the discharge zone of the karst aquifer on the hydraulic conditions (flow velocities, flow rates, and conduit-matrix interaction in the conduit network and matrix).
- To evaluate the impact of the thickness and permeability of a cover layer on karst drainage patterns and its drainage behaviour.

A simplified 3D conceptual model with different settings was developed and numerically tested to achieve these objectives.

2 | METHODOLOGY

In this study, a simplified representation of a karst system is created using a schematized conceptual model, which includes aquifer properties, hydrogeological boundaries, recharge and discharge mechanisms and other relevant parameters. The schematic model is used to illustrate the main components of the system and their relationships. Numerical simulations are then conducted to test the plausibility of the basic hydrogeologic assumptions.

2.1 | Description of the model scenarios

We investigated the hydrologic impacts of sediment deposition, resulting from a base level rise, on the discharge zone of the karst

aquifer. Our study utilized six different model configurations incorporating sediment covers varying in thickness and permeability. (see Figure 1). These configurations include:

- (a) Represents the reference configuration with flow through the aquifer system without discharge through karst conduits. This configuration quantifies the influence of conduit networks in the other configurations.
- (b) Represents the initial state before a positive base level shift and sediment deposition on the discharge zone, with karst drainage primarily through the main conduit network.
- (c) Incorporates a thin sediment cover (20 m) on the discharge zone consisting of highly permeable unconsolidated deposits. (10^{-2} m/s), such as fluvial sand to gravel deposits.
- (d) Incorporates a thin sediment cover (20 m) on the discharge zone consisting of low permeable sediments (10^{-8} m/s) such as silt or loess.
- (e) Incorporates a thick sediment cover (50 m) on the discharge zone consisting of the highly permeable unconsolidated sediments described in configuration (c).
- (f) Incorporates a thick sediment cover (50 m) of the discharge zone consisting of the low permeable sediments described in configuration (d).

These configurations enable us to analyse the development of the karst water table, drainage patterns and the interaction between conduits and matrix in karst systems, under varying discharge zone conditions resulting from sediment deposition and base level shifts.

2.2 | Hydrogeological conceptual model

The simplified model represents a hypothetical karst aquifer drained by a Vauclusian-type perennial spring at contact with an impermeable formation acting as a barrier (Figure 2). Its geometry roughly corresponds to those of karst systems on the southern edge of the Swabian Alb (Lauber et al., 2013, 2014; Villinger, 1977; Villinger & Ufrecht, 1989). The model is 21 km long and 10 km wide and assumes Darcy's law governs matrix flow. It comprises four geological units: a karst aquifer with a fractured rock matrix conductivity and a conduit flow capacity/conduit conductivity, an impermeable bedrock, a sedimentary cover layer, and a drainage layer on top of the sediments, required by the model geometry to drain the water out. The karst aquifer has a constant thickness of 140 m and a catchment area of 150 km². A karst groundwater recharge of 200 mm/a results in a total spring discharge rate of 0.95 m³/s. The hydraulic conductivity of the karst rock matrix, including smaller fissures and fractures, is 5×10^{-5} m/s. The spring is fed by a hierarchically organized karst conduit system has a branchwork pattern and high conductivity and is located at the aquifer base, divided into three conduit sections increasing in diameter towards the outlet (I, II, III).

Note: Natural karst systems are highly complex and variable, which makes it challenging to capture all aspects of flow transport,

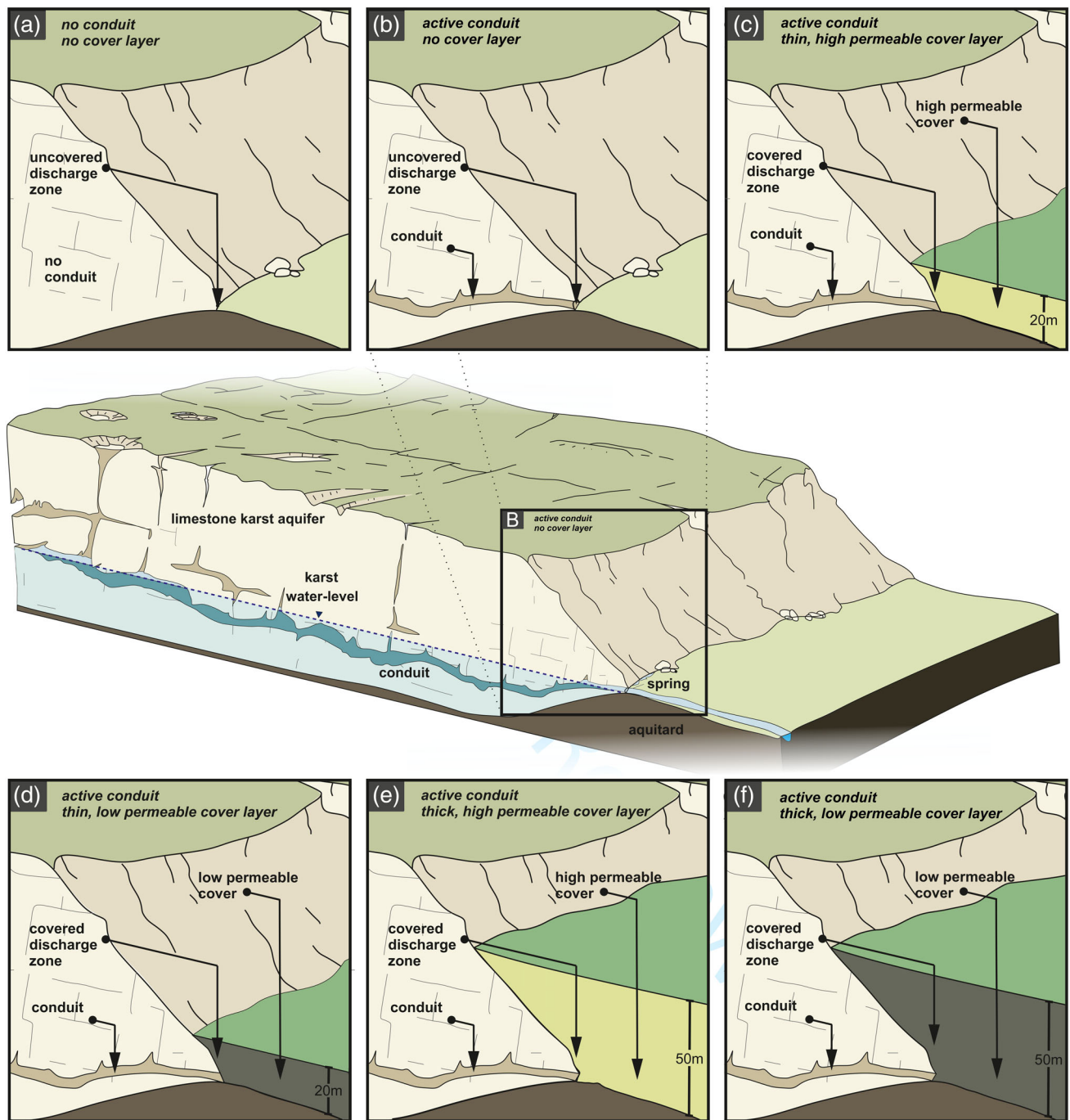


FIGURE 1 Six model configurations (a–f) were utilized in this study to investigate the impact of sediment coverage on the karst drainage discharge zone, as depicted in the schematic overview.

especially in heterogeneous environments. The behaviour of karst aquifers is influenced by various factors such as rock porosity, bedding, jointing, recharge through epikarst and unsaturated zone, and speleogenetic processes. However, these factors may not or only partially be represented in the simplified conceptual model used in this study. Therefore, it is essential to recognize and account for the limitations and uncertainties when interpreting the results of conceptual models.

2.3 | Groundwater flow model

This study utilized FEFLOW 7.3, a finite element groundwater modelling software by DHI WASY (Diersch, 2014), to create a steady-state groundwater flow model. The model consists of 14 slices, each containing 455 103 elements, representing a complete catchment area of a karst spring. A no-flow boundary condition was applied along the model boundary, and the total groundwater recharge ($84\,000\text{ m}^3/\text{d}$)

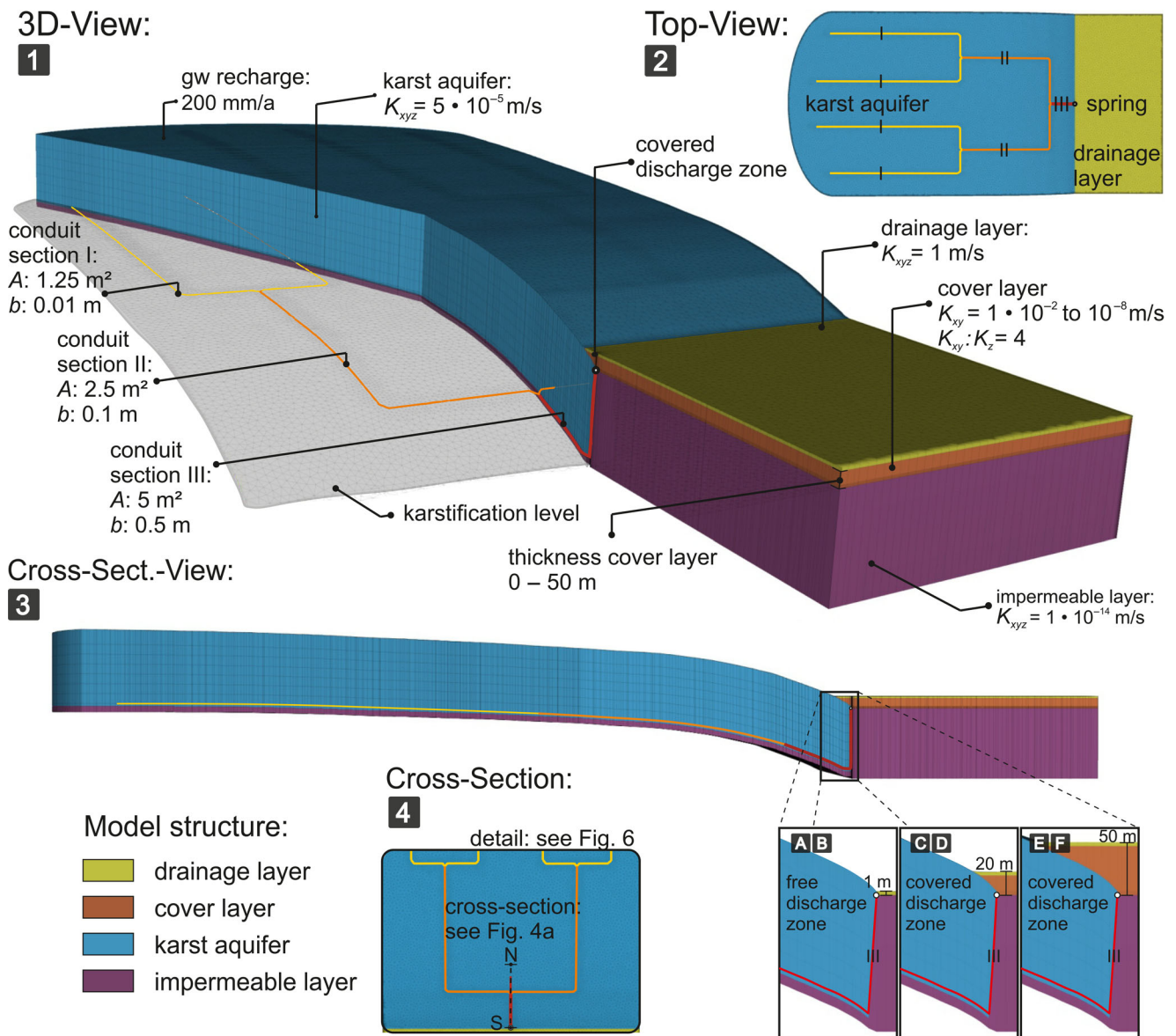


FIGURE 2 The schematic overview of the numerical FEFLOW model domain includes the following features and parameters. 1: 3D view with the clipping plane and view of the conduit network. 2: model domain from above. 3: Model cross-section along the main conduit, that shows the discharge zone with different cover thicknesses of the configurations (a–f). 4: Top view of the cross-section shown in Figure 4 and section of Figure 6.

comes from recharge into the model from the top of the karst layer. The base-level was set with a specific head boundary condition according to six configurations A–F at the model outlet to represent the discharge in this elevation. The model neglects hydrodynamic and flow processes in soil, epikarst, and speleogenetic processes. A conduit network was embedded in the model with 880 1D discrete feature elements. Fluid conductivity is higher in the elements representing conduits than in the surrounding porous medium, and they are connected to the porous medium at model nodes. Hydraulic interactions between the two occur at these nodes. The conduit network is modelled using the Hagen-Poiseuille law, which calculates the average velocity of laminar flow in one-dimensional conduits.

The discharge rate of a single conduit with cross-sectional area A_c can be expressed as:

$$Q = A_c \bar{v} = \pi r^2 \frac{r^2 \rho g \bar{l}}{8\mu} \quad (1)$$

here, r is the conduit radius, ρ is the fluid density, g is the acceleration due to gravity, μ is the fluid's kinematic viscosity, and \bar{l} is the unit vector in the direction of flow, $r^2/8$ represents conduit permeability, and $r^2\pi$ represents conduit cross-section. In numerical modelling, conduit conductivity with hydraulic aperture $b = 2r$ is expressed as:

$$K_c = A_c K = \frac{\pi b^4 \rho g}{128 \mu} \quad (2)$$

The hydraulic apertures b for conduit Sections I, II, and III are 0.01, 0.1, and 0.5 m, respectively. The Hagen-Poiseuille equation assumes laminar flow in a round conduit with smooth walls, and that the flow is steady-state and incompressible.

This is sufficient to drain the entire recharge through the conduit. The conduit network is fully located within the phreatic zone due to its position below the spring level. The governing balance equations for discrete features can be found in the literature Diersch (2014). Although some parts of the conduit network in several model configurations are in the transitional range between laminar and turbulent fluid flow based on the Reynolds number, we used the Hagen-Poiseuille equation due to the model's conceptual nature. While this may introduce uncertainty, we believe it will not significantly impact the results and acknowledge the need to remain aware of this potential limitation.

3 | RESULTS

3.1 | Impact on conduit flow rates

Figure 3 depicts the relationship between simulated conduit discharge in conduit Section II/III and the thickness and hydraulic conductivity of sediments covering the discharge zone. The left panel (1) shows

the effect of a 20 m thick sediment layer, while the right panel (2) the effect of a 50 m thick cover layer. The hydraulic conductivity of the deposits is systematically decreased from 10^{-2} m/s (blue line) to 10^{-8} m/s (red line). The black line represents the initial free-draining spring discharge. The two middle panels provide information about the locations of conduit flow changes within the model. The blue area represents the uncovered karst, while the yellow area is the karst covered by sediments. The discharge of the free-draining spring is about 900 L/s, representing 90.5% of the total recharge. Results demonstrate that overlaying the conduit outlet with a 20-m thick layer of a material with high hydraulic conductivity, such as gravel with a K value of 10^{-2} m/s, can effectively reduce spring discharge (i.e., seepage of water from the conduit into the deposits) by more than 50%. A deposit of fine sandy (10^{-3} m/s) or finer material with the same thickness would almost completely plug the buried spring. The rapid decrease in conduit discharge within a distance of less than 1 km from the spring location indicates that a significant amount of impounded water is drained into the rock matrix before reaching the surface. If present, the back flooding could lead to a reactivation of paleo conduits and spring, or cause potential new preferential flow paths such as along faults and bedding planes, leading to the emergence of water at discharge points on the edge of uncovered karst to covered karst. In model configurations with a 50-m-thick sediment cover, a nearly linear decline in conduit discharge is evident at distances below 4 km from the outlet. Across all configurations, sediment has a discernible effect on flow rate up to a distance of approximately 7 km from the outlet.

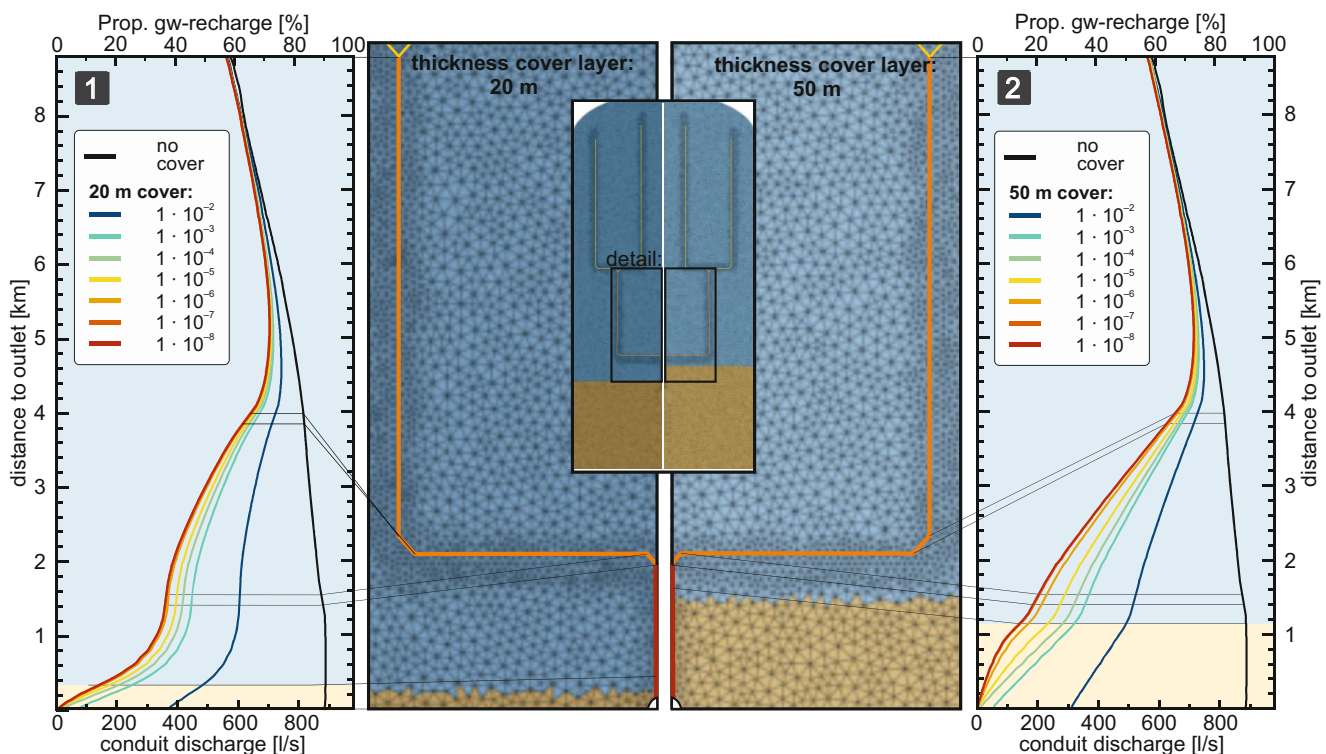


FIGURE 3 Discharge in conduit II/III with unaffected drainage on the outlet (black line) and with discharge zone sediment cover with thicknesses of 20 m (1) and 50 m (2). The hydraulic conductivity of the cover layer varies between 10^{-2} and 10^{-8} m/s. Blue area: uncovered karst; yellow area: karst covered by deposits.

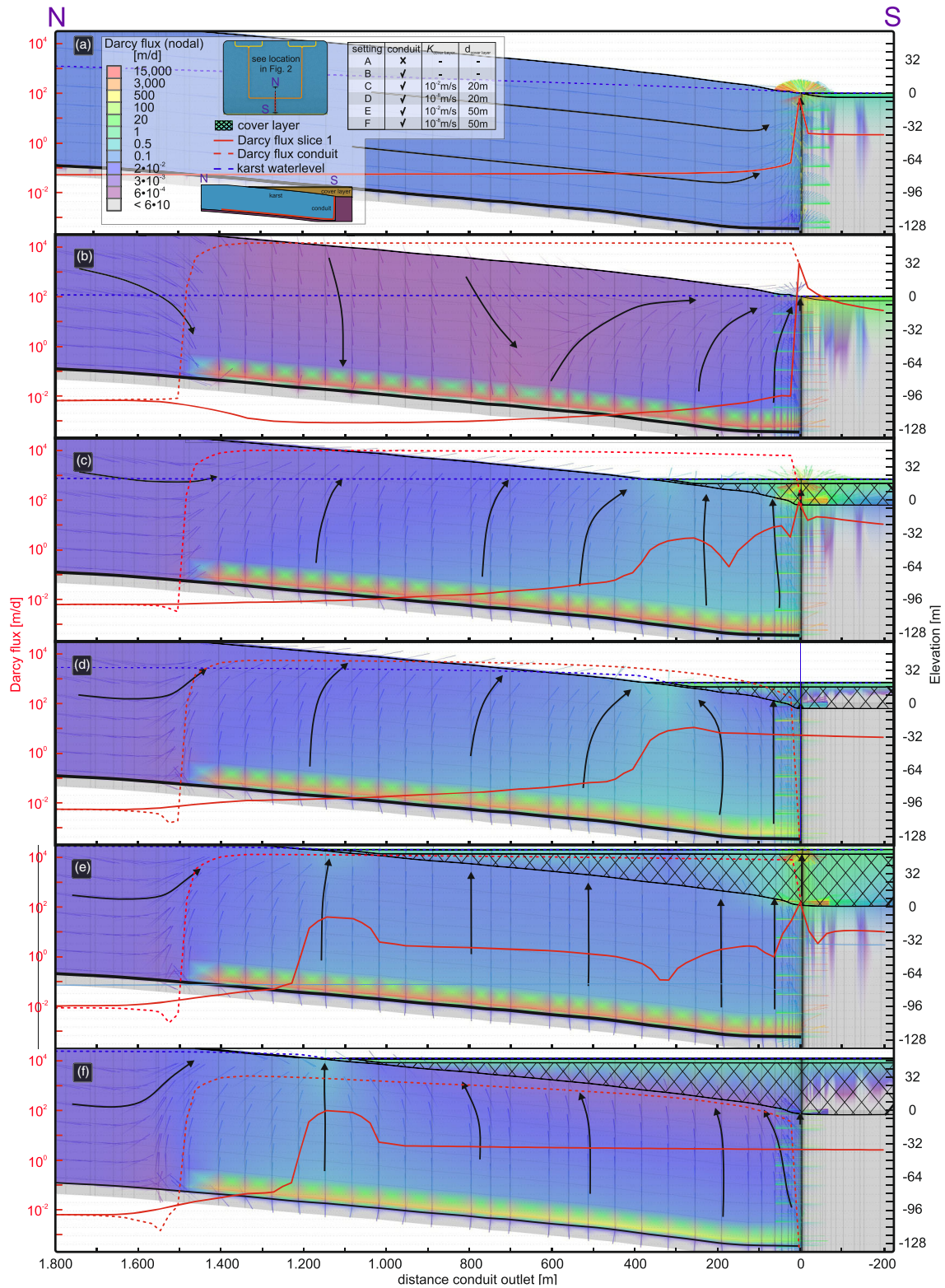


FIGURE 4 Nodal Darcy flux distribution along a cross-section. The solid red line represents the conduit Darcy flux in the conduit. The red dashed line is the Darcy flux in the matrix of the top model slice, and the blue line shows the karst water table. Arrows display the Darcy flux flow pattern. The location of the cross-section is shown in Figure 4.

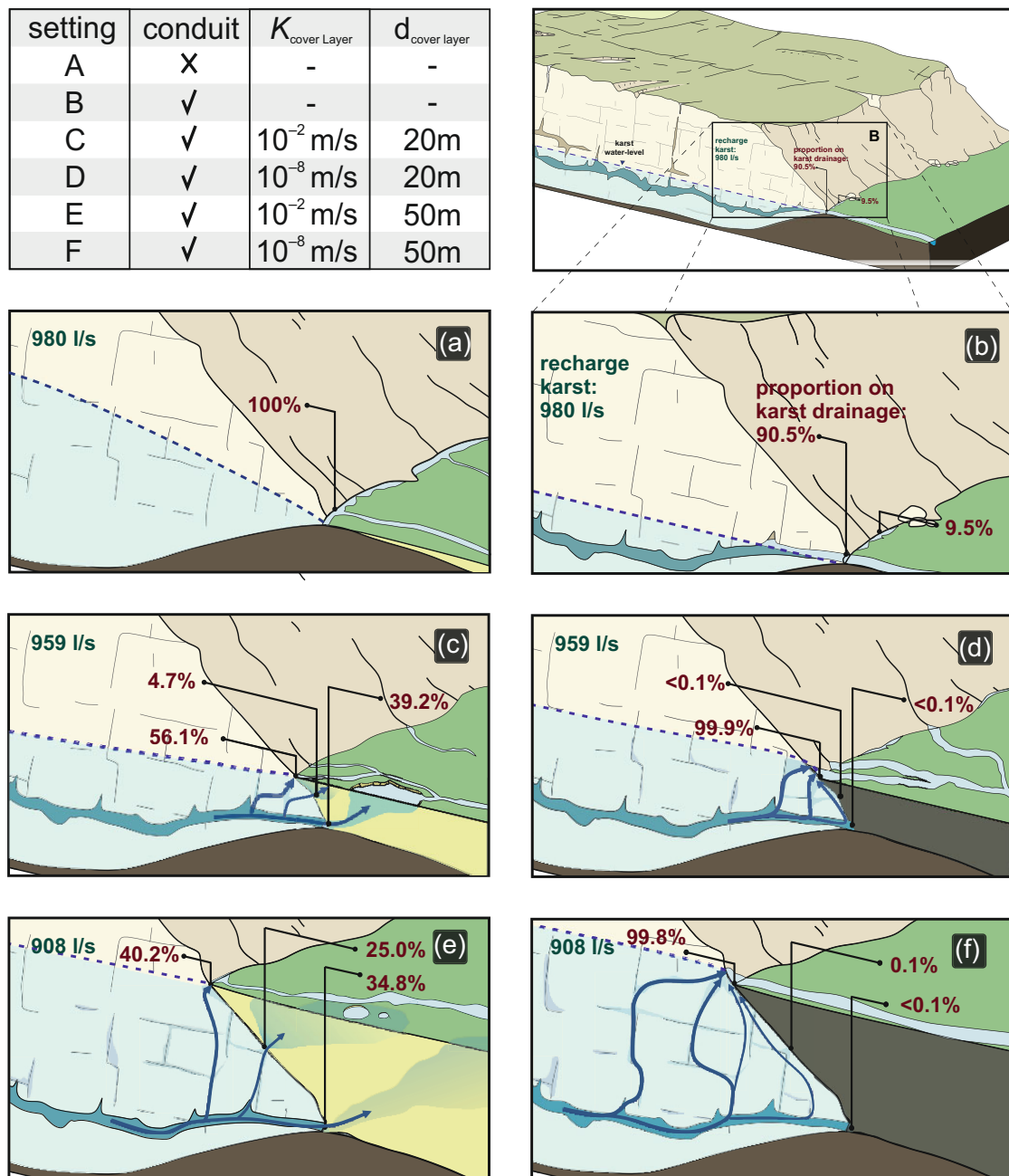


FIGURE 5 Influence of a cover layer (with different thicknesses and permeability) covering the drainage zone on the development of flow patterns, including the proportion of preferential flow paths in the total discharge. The difference in groundwater recharge results from the decrease in exposed karst surface area due to the sediments.

3.2 | Impact on conduit matrix interaction

Figure 4 presents a line plot/cross-section view of the Darcy flux section N–S for six different model configurations (a–f). The red dashed line represents the Darcy flux in the conduit, while the solid red line shows the Darcy flux in the top model slice, indicating water exchange from the karst into the sediments or surface. The blue dashed line represents the potentiometric groundwater surface, which shows artesian conditions if above the model surface or if water reaches the surface. The background colours illustrate the Darcy flux

in the conduit and the matrix in a cross-sectional view of the model domain of the 3D model. The comparison between inactive (A) and active conduit (B) systems highlights the crucial role of the conduit system in karst drainage. The conduit discharges 90.5% of the recharge (see Figure 3). This is also reflected by the significantly lower matrix flux of 9.5×10^{-4} m/d compared to inactive conduit setting A with 7.5×10^{-2} m/d. The flow direction changes from a slope-parallel flow (a) to a radial flow towards the conduits (b). At a horizontal distance of 600 m from the conduit outlet, the flow field changes again from a downward flow towards the conduit to an upward flow

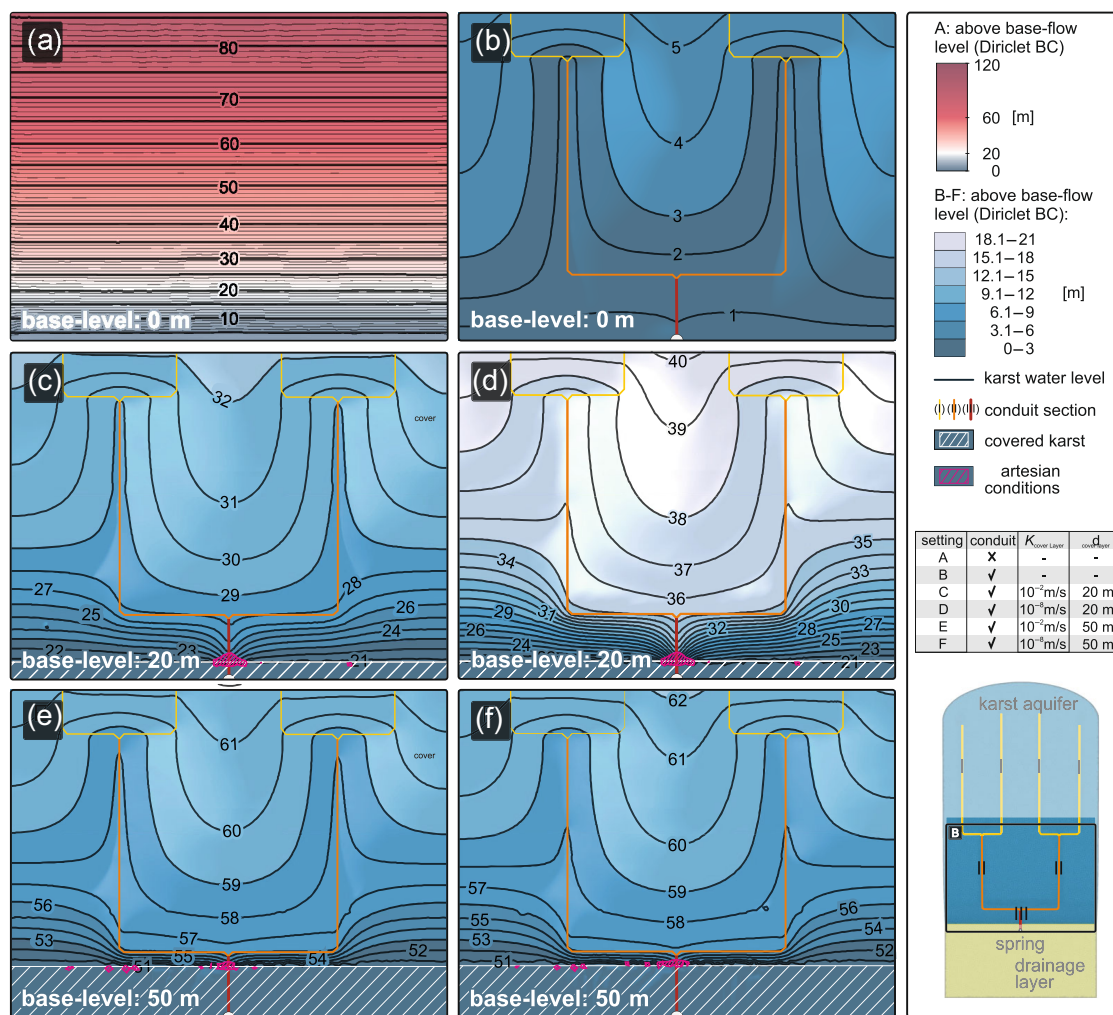


FIGURE 6 Simulated (steady-state) piezometric karst surface of the 6 model configurations applied in the study.

towards the ground surface. As the thickness of the deposits increases and the permeability decreases (c–f), the Darcy flux in the conduit decreases significantly, and more water is pushed from the conduit into the matrix due to increasing water pressure within the conduits. In both configurations with a low permeable sediment cover (d, f), the water pressure led to artesian conditions within the karst layer (blue dashed line above the model surface).

3.3 | Impact on drainage patterns

Figure 5 illustrates the discharge conditions, namely conduit outlet, geological contact karst aquifer with sediment cover, and contact karst aquifer with the model top, for each of the six model configurations examined. The presence of a thin, highly permeable layer (c) leads to the development of a dominant dual flow path regime. Here, 39.2% of the conduit discharge drains from the buried conduit outlet into the sediments and then rises vertically to the surface, while 56.1% reaches the surface directly from the karst matrix at the contact zone with the sediments. The remaining 4.7% enters the

sediments laterally below ground from the karst matrix. The figures presented here are qualitative and based on a defined hydraulic conductivity of the karst matrix at 5×10^{-5} m/s. However, it is important to recognize that this value may be higher than the observed hydraulic conductivity in many actual karst systems.

Increasing the thickness of the cover layer (e) without changing K results in a shift in the drainage pattern. As the base level rises and the contact area with the sediment increases, diffuse lateral exchange through the sediments becomes more prevalent (4.7% → 25.0%). The proportion of the conduit discharge decreases comparatively less than the direct discharge at the interface (39.2%–34.8% vs. 56.1%–40.2%, respectively).

As the hydraulic conductivity of the cover layer decreases, the outlet becomes increasingly plugged, and at hydraulic permeabilities observed in (d) and (f), it becomes entirely plugged (<0.1%). This causes the water trapped in the conduit to be forced upwards into the matrix, resulting in artesian conditions within the covered karst. There is also almost no diffusive exchange through the sediments (<0.1%). In actual karst systems, this condition is unlikely to persist for long due to the significant gradient. In such cases, existing

paleo-phreatic levels or overflow springs may reactivate, and fractures or faults in the area may result in the formation of new conduits where water can rise and create a Vauclusian-type artesian spring.

3.4 | Impact on karst water table

The simulated steady-state karst water table of the six model configurations (a–f) is shown in Figure 6. In all configurations with an existing conduit (b–f), the conduit functions as the primary drainage network with a strong interaction between the conduit and matrix. In conduit Section I and the upper part of conduit Section II, the conduit acts as a drain from the surrounding matrix. The gradient reverses in the further course towards the outlet, causing water to flow from the conduit into the matrix. Even with a fully plugged outlet (f), the karst water table remains below the level that would develop with a lower base level and without a conduit (a). In configuration (b), the phreatic zone starts only slightly above the conduit level.

Real karst systems are known to exhibit significant and rapid fluctuations in water levels during periods of high recharge or low discharge, due to their high permeability and limited storage capacity. However, the behaviour of aquifers can vary widely depending on the local geology and hydrology of the system and many natural systems swap somehow between case b (low water) and cases c–f during high water conditions, when their outlet is too small compared to the incoming discharge rate.

4 | CONCLUSIONS

In this study, we developed numerical testing of a conceptual karst model to examine how sediment coverage affects karst drainage when sedimentation in the discharge zone is faster than speleogenetic processes. We tested six different sediment configurations with varying thickness and hydraulic conductivity and found that even a thin cover of highly hydraulic conductive sediments ($K = 10^{-2}$ m/s) reduces conduit outlet discharge by more than half.

A less permeable sediment cover completely plugs the outlet, resulting in its full inactivation. However, even with an impervious sediment cover, the conduit system remains crucial to karst drainage because it gathers water from the recharge zone and carries it towards the buried outlet. The reduced drainage of the outlet creates high pressure, which causes water to flow upwards into the matrix. In this scenario, lateral or horizontal water exchange with the sediments is insignificant. We observed artesian conditions in the geological contact area. This can result in the reactivation of paleo conduits or the emergence of water through faults and bedding zones. Covering the outlet of a mature conduit system with low permeability sedimentary cover will inevitably cause a considerable rise in the karst water table, leading to the formation of new conduits and Vaucluse-type springs in the contact zone between the limestone and the sediments.

In the case of a thin, highly permeable sediment layer, we observe significant vertical hydraulic exchange with the karst aquifer, resulting in

a dominant dual flow system. Similarly, covering the conduit outlet in this scenario will impound the karst water to the level of the karst-sediment interface. Existing water pathways will be used for flow transport, resulting in the majority of karst drainage occurring at new springs that emerge at the interface. In the second flow path, water from the active, buried karst cave enters the sediments and rises vertically within a discrete zone, appearing as a large limnocene spring. A smaller part of the discharge enters the karst matrix via a third flow path from the conduit. From there, it enters the sediments laterally, diffusely. Increasing the thickness of the sediment cover without changing K results in more water exiting along the third flow path. The results of the simulations with a highly permeable sediment cover agree in many respects with the observations of the PSS (Petitta et al., 2015) and the karst-gravel-aquifer interaction in the Donauried (Fahrmeier et al., 2022), both mentioned in the introduction section, resp. support the hypotheses that buried karst conduits (or highly fractured zones) are present there.

Karst aquifers exhibit rapid water level fluctuations due to high permeability and limited storage capacity. Aquifer behaviour varies depending on local geology and hydrology. Existing karst systems can switch between low and high water conditions, such as from case b to cases c–f during high water when the outlet is too small compared to incoming discharge rates. Understanding these dynamics is crucial for managing karst aquifers and their water resources.

ACKNOWLEDGEMENTS

The authors would like to thank Prof. Ty Ferré for his valuable edits, suggestions, and language and grammar check. This study is a contribution to the research project karst Aquifer Resources availability and quality in the Mediterranean Area (KARMA project, grant agreement number 01DH19022A). Open Access funding enabled and organized by Projekt DEAL.

DATA AVAILABILITY STATEMENT

Data sharing not applicable to this article as no datasets were generated or analysed during the current study.

ORCID

Marc Ohmer  <https://orcid.org/0000-0002-2322-335X>

REFERENCES

- Abusaada, M., & Sauter, M. (2013). Studying the flow dynamics of a karst aquifer system with an equivalent porous medium model. *Ground Water*, 51(4), 641–650.
- Audra, P., Mocochain, L., Camus, H., Gilli, E., Clauzon, G., & Bigot, J.-Y. (2004). The effect of the Messinian deep stage on karst development around the Mediterranean Sea. Examples from Southern France. *Geodinamica Acta*, 17(6), 389–400.
- Bakalowicz, M. (2005). Karst groundwater: A challenge for new resources. *Hydrogeology Journal*, 13(1), 148–160.
- Bednar, D., Jr. (2000). Speleogenesis: Evolution of karst aquifers. *Journal of Hydrology*, 240(1–2), 145–146.
- Berglund, J. L., Toran, L., & Herman, E. K. (2020). Can karst conduit models be calibrated? A dual approach using dye tracing and temperature. *Groundwater*, 58(6), 924–937.
- Bonacci, O. (2001). Analysis of the maximum discharge of karst springs. *Hydrogeology Journal*, 9(4), 328–338.

- Bresinsky, L., Kordilla, J., Thoenes, E., Würsch, T., Engelhardt, I., & Sauter, M. (2020). Simulating Climate Change Impacts on the Recharge Dynamics of a Mediterranean Karst Aquifer. Technical report.
- Chen, Z., & Goldscheider, N. (2014). Modeling spatially and temporally varied hydraulic behavior of a folded karst system with dominant conduit drainage at catchment scale, Hochifèn–Gottesacker, Alps. *Journal of Hydrology*, 514, 41–52.
- Diersch, H.-J. G. (2014). *FEFLOW: Finite element modeling of flow, mass and heat transport in porous and fractured media* (1st ed.). Springer Berlin Heidelberg: Imprint: Springer.
- Dreybrodt, W. (1990). The role of dissolution kinetics in the development of karst aquifers in limestone: A model simulation of karst evolution. *The Journal of Geology*, 98(5), 639–655.
- Fahrmeier, N., Frank, S., Goepfert, N., & Goldscheider, N. (2022). Multi-scale characterization of a complex karst and alluvial aquifer system using a combination of different tracer methods. *Hydrogeology Journal*, 30, 1863–1875.
- Fahrmeier, N., Goepfert, N., & Goldscheider, N. (2021). Comparative application and optimization of different single-borehole dilution test techniques. *Hydrogeology Journal*, 29(1), 199–211.
- Fiasca, B., Stoch, F., Olivier, M.-J., Maazouzi, C., Petitta, M., Di Cioccio, A., & Galassi, D. M. (2014). The dark side of springs: What drives small-scale spatial patterns of subsurface meiofaunal assemblages? *Journal of Limnology*, 73(1), 71–80.
- Ford, D., & Williams, D. (2007). *Karst hydrogeology and geomorphology*. John Wiley & Sons Ltd.
- Frank, S., Goepfert, N., Ohmer, M., & Goldscheider, N. (2019). Sulfate variations as a natural tracer for conduit-matrix interaction in a complex karst aquifer. *Hydrological Processes*, 33(9), 1292–1303.
- García-Castellanos, D., Estrada, F., Jiménez-Munt, I., Gorini, C., Fernández, M., Vergés, J., & De Vicente, R. (2009). Catastrophic flood of the Mediterranean after the Messinian salinity crisis. *Nature*, 462(7274), 778–781.
- García-Castellanos, D., Micallef, A., Estrada, F., Camerlenghi, A., Ercilla, G., Perriáñez, R., & Abril, J. M. (2020). The Zanclean megaflood of the Mediterranean – Searching for independent evidence. *Earth-Science Reviews*, 201, 103061.
- Ghasemizadeh, R., Yu, X., Butscher, C., Hellweger, F., Padilla, I., & Alshawabkeh, A. (2015). Equivalent porous media (EPM) simulation of groundwater hydraulics and contaminant transport in karst aquifers. *PLoS One*, 10(9), e0138954.
- Glennon, A., & Groves, C. (2002). An examination of perennial stream drainage patterns within the Mammoth Cave watershed, Kentucky. *Journal of Cave and Karst Studies*, 64(1), 82–91.
- Goldscheider, N. (2019). A holistic approach to groundwater protection and ecosystem services in karst terrains. *Carbonates and Evaporites*, 34(4), 1241–1249.
- Green, R. T., Painter, S. L., Sun, A., & Worthington, S. R. H. (2006). Groundwater contamination in karst terranes. *Water, Air, & Soil Pollution: Focus*, 6(1–2), 157–170.
- Hartmann, A., Goldscheider, N., Wagener, T., Lange, J., & Weiler, M. (2014). Karst water resources in a changing world: Review of hydrological modeling approaches. *Reviews of Geophysics*, 52(3), 218–242.
- Jeannin, P.-Y. (2001). Modeling flow in phreatic and epiphreatic karst conduits in the Hölloch Cave (Muotatal, Switzerland). *Water Resources Research*, 37(2), 191–200.
- Kavouri, K., & Karatzas, G. P. (2016). Integrating diffuse and concentrated recharge in karst models. *Water Resources Management*, 30(15), 5637–5650.
- Kiraly, L. (1998). Modelling karst aquifers by the combined discrete channel and continuum approach. *Bulletin du Centre d'Hydrogeologie*, 16, 77–98.
- Kolokotronis, V., Plum, H., Schloz, W., & Rausch, R. (2002). Hydrogeologische Karte von Baden-Württemberg. Ostalb. Erläuterungen. Technical report, Landesamt für Geologie, Rohstoffe und Bergbau Baden-Württemberg; Landesanstalt für Umweltschutz, Baden-Württemberg, Freiburg, Karlsruhe.
- Kordilla, J., Sauter, M., Reimann, T., & Geyer, T. (2012). Simulation of saturated and unsaturated flow in karst systems at catchment scale using a double continuum approach. *Hydrology and Earth System Sciences*, 16(10), 3909–3923.
- Kovács, A., & Sauter, M. (2007). Modelling karst hydrodynamics. In *Methods in Karst Hydrogeology*. Taylor and Francis.
- Lakušić, S. (2018). Application of artificial neural networks for hydrological modelling in Karst. *Journal of the Croatian Association of Civil Engineers*, 70(1), 1–10.
- Lauber, U., Ufrect, W., & Goldscheider, N. (2013). Neue Erkenntnisse zur Struktur der Karstentwässerung im aktiven Höhlensystem des Blautopfs. *Grundwasser*, 18(4), 247–257.
- Lauber, U., Ufrect, W., & Goldscheider, N. (2014). Spatially resolved information on karst conduit flow from in-cave dye tracing. *Hydrology and Earth System Sciences*, 18(2), 435–445.
- Liesch, T., Wunsch, A., Chen, Z., & Goldscheider, N. (2021). Modeling the discharge behavior of an alpine karst spring influenced by seasonal snow accumulation and melting based on a deep-learning approach. other, pico.
- Mocochain, L., Audra, P., & Bigot, J.-Y. (2011). Base level rise and per ascensum model of speleogenesis (PAMS). Interpretation of deep phreatic karsts, vauclisian springs and chimney-shafts. *Bulletin de la Société Géologique de France*, 182(2), 87–93.
- Ninanya, H., Guiguer, N., Vargas, E. A., Nascimento, G., Araujo, E., & Cazarin, C. L. (2018). Analysis of water control in an underground mine under strong karst media influence (Vazante mine, Brazil). *Hydrogeology Journal*, 26(7), 2257–2282.
- Paleologos, E. K., Skitzi, I., Katsifarakis, K., & Darivianakis, N. (2013). Neural network simulation of spring flow in karst environments. *Stochastic Environmental Research and Risk Assessment*, 27(8), 1829–1837.
- Panday, S., Langevin, C., Niswonger, R., Ibaraki, M., & Hughes, J. (2013). MODFLOW-USG Version 1: An Unstructured Grid Version of MODFLOW for Simulating Groundwater Flow and Tightly Coupled Processes Using a Control Volume Finite-Difference Formulation, volume book 6, chap. A45. U.S. Geological Survey Techniques and Methods. Series: Techniques and Methods.
- Peleg, N., & Gvirtzman, H. (2010). Groundwater flow modeling of two-levels perched karstic leaking aquifers as a tool for estimating recharge and hydraulic parameters. *Journal of Hydrology*, 388(1–2), 13–27.
- Petitta, M., Caschetto, M., Galassi, D. M. P., & Aravena, R. (2015). Dual-flow in karst aquifers toward a steady discharge spring (Presciano, Central Italy): Influences on a subsurface groundwater dependent ecosystem and on changes related to post-earthquake hydrodynamics. *Environmental Earth Sciences*, 73(6), 2609–2625.
- Scanlon, B. R., Mace, R. E., Barrett, M. E., & Smith, B. (2003). Can we simulate regional groundwater flow in a karst system using equivalent porous media models? Case study, Barton Springs Edwards aquifer, USA. *Journal of Hydrology*, 276(1–4), 137–158.
- Schloz, W., Armbruster, V., Prestel, R., & Weinzierl, W. (2007). Hydrogeologisches Abschlussgutachten zur Neuabgrenzung des Wasserschutzgebietes Donauried-Hürbe für die Fassungen des Zweckverbandes Landeswasserversorgung im württembergischen Donauried und bei Giengen-Burgberg. Technical report, Landesamt für Geologie Rohstoffe und Bergbau, Regierungspräsidium Freiburg.
- Shoemaker, W., Kuniansky, E., Birk, S., Bauer, S., & Swain, E. (2008). Documentation of a Conduit Flow Process (CFP) for MODFLOW-2005. Techniques and Methods, U.S. Geological Survey Techniques and Methods. Series: Techniques and Methods.
- Udluft, P. (Ed.). (2000). Das Grundwasser im schwäbischen Donautal: hydrologisch-hydrogeologische Untersuchung mit Erstellung eines Grundwassermodells im Maßstab 1: 25 000/50 000 im Donautal zwischen Ulm/Neu-Ulm und Neuburg an der Donau. Number 11 in Schriftenreihe der Bayerischen Sand- und Kiesindustrie. Bayerischer

Industrieverband Steine und Erden, Fachabt. Sand- und Kiesindustrie, München.

- Villinger, E. (1977). *Über Potentialverteilung und Strömungssysteme im Karstwasser der Schwäbischen Alb (Oberer Jura, SW-Deutschland)*. Schweizerbart Science Publishers.
- Villinger, E., & Ufrecht, E. (1989). Ergebnisse neuer Markierungsversuche im Einzugsgebiet des Blautopfs (mittlere Schwäbische Alb). *Mitteilungen des Verbandes der deutschen Höhlen- und Karstforscher*, 35, 25–38.

How to cite this article: Ohmer, M., Liesch, T., & Goldscheider, N. (2023). Influence of sediments burying the discharge area of a karst aquifer on the groundwater flow field—Numerical testing of conceptual models. *Hydrological Processes*, 37(12), e15048. <https://doi.org/10.1002/hyp.15048>